Modeling Emitter Breakdown in GaAs-Based HBTs

M. Rudolph, F. Schnieder, W. Heinrich

Ferdinand-Braun-Institut für Höchstfrequenztechnik (FBH),
Albert-Einstein-Str. 11, D-12489 Berlin, Germany. E-mail: m.rudolph@ieee.org

Abstract— **Emitter breakdown is commonly ignored in compact HBT models. However, it can have a significant impact on the HBT power performance. The aim of this paper is to present a compact model that accounts for the effect. It is validated by load-pull measurements and applied to investigate the electro-thermal interaction in multi-finger HBTs.**

I. Introduction

Avalanche breakdown is one of the factors that limit GaAs HBT power performance. Hence, a lot of work has been spent on modeling the base-collector breakdown [1], [2], [3]. In forward operation, this junction is reverse-biased while carrying the collector current, therefore, avalanche breakdown is expected to occur at this junction rather than at the base-emitter junction. However, relatively high breakdown voltages are easily achieved in GaAs collectors, therefore the collector breakdown often is of minor importance in power applications, in case of mobile applications with 3 V supply voltage as well as for base station devices that operate with supply voltages of 27 V.

On the other hand, emitter breakdown is commonly ignored in compact models, since the base-emitter junction is usually forward biased. This assumtion may not hold, if the HBT is biased in class AB or B and is driven by relatively high powers, while the base bias is supplied by a high-impedance source. In this case, the voltage swing can reach deep into the negative region. Also, the base-emitter junction breakdown voltage is commonly low compared to the base-collector one. Biasing the HBT at low quiescent currents is important not only to reduce power consumption, but sometimes also to prevent thermal destruction of the device due to self-heating. A low-impedance base bias supply in contrast can lead to destruction of the HBT due to thermal feedback. Proper design of the bias circuit is therefore crucial for these two reasons, emitter breakdown and self-heating, and the model should be capable to help the designer to avoid breakdown.

While characterizing the HBTs, however, bias usually is supplied by almost perfect stabilized sources. Therefore the emitter breakdown may artificially limit the HBT power performance in a way that will not be observed in a more realistic circuit set-up.

In this paper, we will first introduce the breakdown model for a HBT unit cell, and point out the impact of this effect on load-pull measurement. The model then is applied to investigate a multi-finger power cell operating at 26 V. Several single-finger large-signal models are combined in order to describe the thermal current crunching behaviour. The interaction of self-biasing, current crunching and emitter breakdown in power operation is investigated.

II. HBT Model

Unlike in case of collector breakdown, emitter breakdown cannot be modeled by a current multiplication factor. This is due to the fact that the emitter breakdown occurs when the HBT is operated in off-state, with negative bias at both junctions and corresponding extremely low currents. Instead, the SPICE model for the similar case of diode breakdown is adopted [4]. A breakdown current source is added in parallel to the base-emitter junction, as shown in Fig. 1:

$$I_{\mathrm{av,e}} = I_f \left(e^{(-V_{\mathrm{ebo}} - V_{\mathrm{be}})/V_{\mathrm{th}}} - 1 \right) \qquad (1)$$

with the base-emitter saturation current I_f, the intrinsic base-emitter voltage V_{be}, the emitter breakdown voltage V_{ebo}, and the thermal voltage V_{th}.

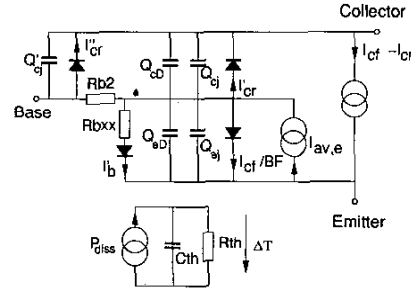

Fig. 1. Intrinsic part of large-signal equivalent circuit.

This breakdown model is included in the FBH HBT model [5], [6], that supports partition of intrinsic and extrinsic base-collector diode, non-ideal base currents, self-heating, current-dependence of base-collector capacitance and collector transit time (i.e. velocity modulation and Kirk effect). In order to calculate the thermal interaction between different emitter fingers inside a multi-finger power cell, the model was extended with regard to the thermal subcircuit shown in Fig. 1. An additional thermal port allows to account for mutual and self-heating of each finger by a thermal resistance matrix.

0-7803-7695-1/03/$17.00 © 2003 IEEE

III. Single-Finger HBT

In this section, the model is applied to a conventional HBT as used e.g. for cell phone handsets [7]. Load-pull measurements are performed at 2 GHz and $V_{CE} = 5$ V with 50 Ω source resistance, and the load is matched in order to achieve maximum output power. Measured and simulated output power and bias points are shown for various biasing conditions in Fig. 2.

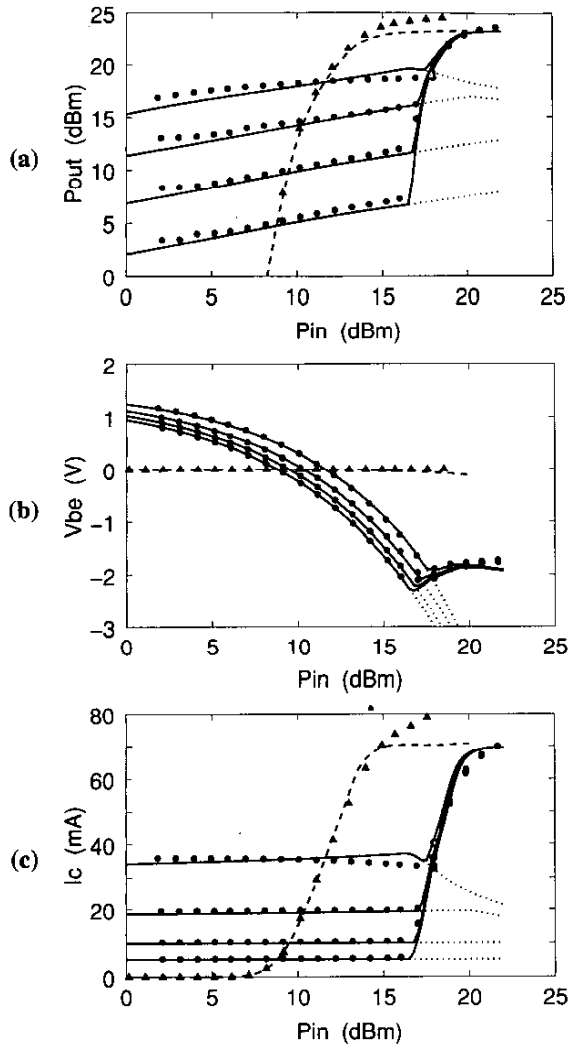

Fig. 2. Bias and output power of unit cell HBT (emitter area $3\times30\,\mu m^2$) at 2 GHz, $V_{CE} = 5$ V, measured (symbols) and simulated (lines) as function of available input power. Constant V_{BE} (- -), constant I_B (—), constant I_B simulated without base-emitter breakdown (· · ·).

When the DC base current I_B is fixed (solid and dotted curves), the output power increases slowly over a wide range of input powers. Beyond a certain limit, above 16 dBm in our case, the output power increases dramatically. In this region, the output power is no longer determined by the quiescent bias point, but all measurements yield the same maximum output power. In this region, it is observed that the DC collector current no longer is proportional to I_B, as one would expect beforehand and as is the case for lower input powers. At the same time, the base-emitter DC voltage V_{BE} reaches a minimum value. This behaviour can be simulated well with the new model including emitter breakdown (solid lines in Fig. 2), while ignoring the breakdown effect leads to significant deviations between measurement and simulation in the second case (dotted lines).

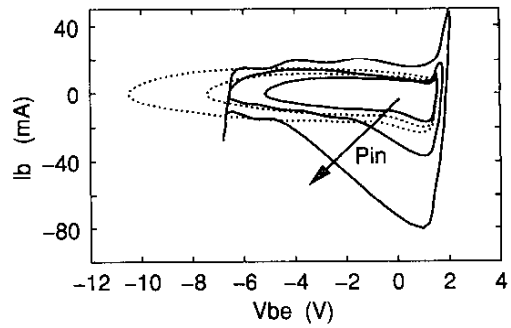

Fig. 3. Base-emitter trajectory of unit cell HBT (emitter area $3\times30\,\mu m^2$) simulated at 2 GHz with (—) and without (· · ·) base-emitter breakdown, $I_B = 0.1$ mA at $P_{in} = 15$, 17.5, and 20 dBm.

The effect of emitter breakdown on the input trajectory is clearly seen in Fig. 3. If a certain limit of input power is reached, the breakdown occurs. On one side, V_{be} can not become lower than the breakdown voltage value (-7 V for our sample). This also limits the DC base-emitter voltage V_{BE} at a value well above the breakdown voltage (Fig. 2b). On the other side, the breakdown renders negative base current swings possible, and consequently the forward mode base current is allowed to increase. The DC value of the total base current is still fixed by the source, but the positive current now is allowed to increase its DC component due to the new conduction part. The collector DC current increases accordingly, since only the positive current component is amplified.

Measurement and simulations performed with constant $V_{BE} = 0$ V are also shown in Fig. 2 (dashed lines). Since V_{BE} is fixed, emitter breakdown is not observed. While no current flows without input power, a steep slope in I_C, I_B and P_{out} is observed once the input power is increased. However, positive thermal feedback can occur. At fixed V_{BE}, I_C increases with temperature which in return increases self-heating. This well known effect can damage the HBT, and a ballasting resistor is required in order to suppress the feedback effect.

In this section, a small transistor was measured at low V_{CE} in order to isolate the breakdown effect from others

such as collector breakdown or thermal current crunching. While the HBT under test was driven very hard and almost above its limits for real life applications, the conclusions drawn from this example also hold for power cells. First of all, the emitter breakdown voltage remains constant independent of the emitter area, therefore one can expect the breakdown to gain importance with larger devices which are operated at higher absolute power levels. Second, the kinks seen in Fig. 2 in P_{out} and bias are a sign for emitter breakdown which would be extremely hard to measure directly in a load-pull measurement. Finally, the model proves to be accurate up to DC currents well beyond the onset of base push-out effect, which is around $I_C = 35\,\text{mA}$ in the present case.

IV. HBT Power Cell

In this section, the model is used to gain insight into the operation of 'high voltage' HBTs designed for base station applications [8]. As an example, a power cell consisting of eight emitter fingers of $3\times70\,\mu\text{m}^2$ is investigated. The HBT has a fishbone type layout, i.e. two rows of four fingers in parallel, as symbolized in the inset in Fig. 4. Thermal management of these transistors is crucial, since they are operated at 27 V up to output powers of 40 dBm. In order to simulate the mutual heating of the individual emitter fingers, each emitter finger is modeled by a single compact transistor model. Thermal interaction is accounted for by a thermal resistance network which is determined beforehand using a numerical thermal simulator [9], [10], [11].

Simulations of the DC IV curves are shown in Fig. 4 for HBTs with thermal shunt air bridges of $5\,\mu\text{m}$ (solid lines) and $20\,\mu\text{m}$ thickness (dashed lines, cf. Fig. 5). Current crunching is observed in case of $5\,\mu\text{m}$ air bridges. The effect that takes place is that half of the HBT is effectively switched off, and hot-spot formation takes place in the middle of the other half (Fig. 4b). Class A operation is not possible in the given case at $V_{CE} = 26\,\text{V}$ for thermal reasons, even if hot-spot formation can be suppressed. In order to investigate the RF performance (Fig. 6), class B or AB biasing has to be applied. Three types of biasing scheme are considered: I_B fixed at 1 mA, and resistances of $50\,\Omega$ and $200\,\Omega$ to ground, ($V_{BE} = 0$ with DC source resistance). The HBT under investigation is the thermally less stable one with the $5\,\mu\text{m}$ air bridges. However, current crunching turns out to be negligible under RF excitation, and is only observed at all near compression when investigating the DC currents through the individual emitter fingers (Fig. 6d). Regarding the biasing scheme, a similar behaviour as in case of the unit cell is observed. Again, emitter breakdown is responsible for the sharp increase of I_C and P_{out} and also limits V_{BE} to values around $-2\,\text{V}$, when I_B is fixed (solid lines). For comparison, simulations without emitter breakdown are shown (dotted lines). In order to avoid thermal damage of the device as well as emitter breakdown, the bias voltage of 0 V is applied through $200\,\Omega$ (dash-dotted lines) and $50\,\Omega$ (dashed lines) resistances. It turns out that in the $200\,\Omega$ case the breakdown is delayed but not suppressed, since the curves show a slight kink around an available input power of 30 dBm, and from here on follow the curves determined with constant I_B. In case of $50\,\Omega$ source resistance, breakdown finally is suppressed at the expense of a only slightly higher I_C and, consequently, dissipated power.

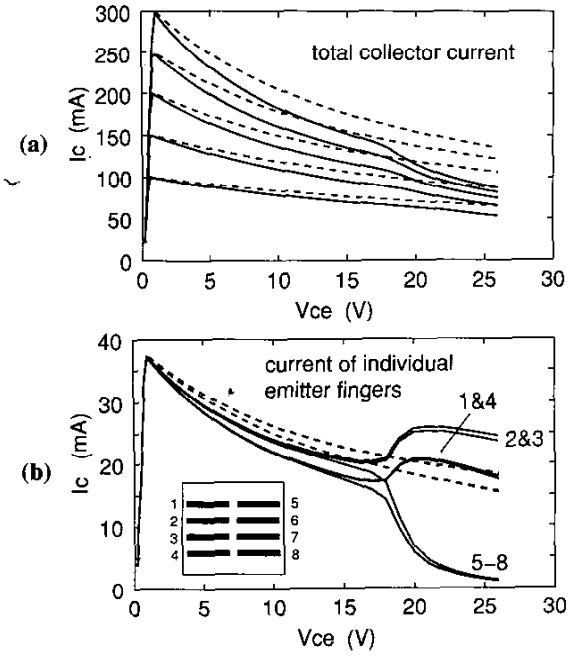

Fig. 4. Simulated DC IV curves of HBT power cell (emitter area $8\,(3\times70)\,\mu\text{m}^2$, fishbone layout as depicted in the lower graph). $5\,\mu\text{m}$ air bridge (—), $20\,\mu\text{m}$ air bridge (- -). **a**: total current, **b**: collector current of individual emitter fingers.

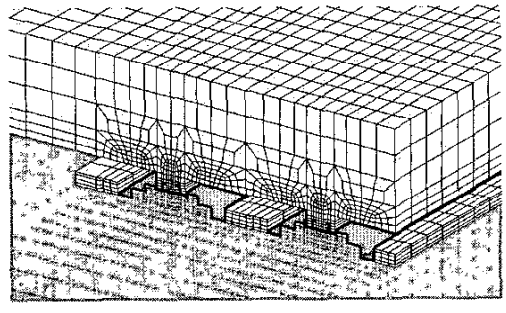

Fig. 5. Cut away of thermal simulation structure, showing two emitter fingers with $20\,\mu\text{m}$ thermal shunt air bridge.

The model gives insight into the complex electro-thermal interaction in HBT power cells even in heavily nonlinear operation and thereby also proves its numerical robustness.

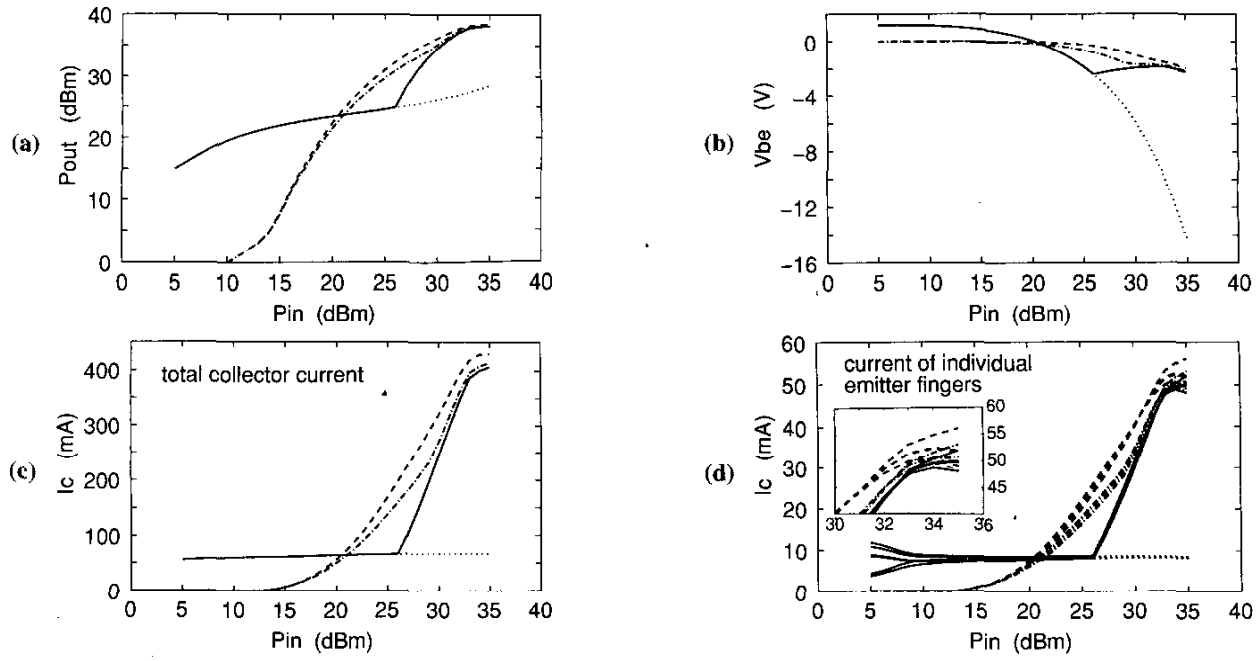

Fig. 6. Bias and output power of HBT power cell (emitter area $8\,(3\times70)\,\mu m^2$, 5 μm air bridge) at 2 GHz, $V_{CE} = 26$ V simulated as function of available input power. Constant I_B (—), constant I_B simulated without base-emitter breakdown (···), $V_{BE} = 0$ with 200 Ω DC source resistance (---), $V_{BE} = 0$ with 50 Ω DC source resistance (- -).

V. Conclusions

The impact of emitter breakdown on HBT power performance is investigated and modeled. It is shown that the effect can lead to self-biasing and increasing collector current despite fixed DC base current. Load-pull measurement and simulations of a HBT unit cell show the enhancement in model accuracy obtained by accounting for emitter breakdown. Moreover the model is used to track the electrothermal interaction in high-power multi-finger HBTs. Mutual heating is accounted for by a thermal resistance matrix which is determined by thermal simulation. The model thereby enhances simulation accuracy of HBT power performance and also proves versatility as a means to analyze thermal management.

Acknowledgments

The authors would like to thank W. Köhler and Dr. P. Heymann for performing the measurements, and the material and process technology departments of the FBH for providing the HBTs.

Financial support by the German BMBF under contract No. 01BM050 is gratefully acknowledged.

References

[1] C.-J. Wei, J. C. M. Hwang, W.-J. Ho, J. A. Higgins, "Large-signal modeling of self-heating, collector transit-time, and RF-breakdown effects in power HBT's," *IEEE Trans. Microwave Theory Tech.*, vol. 44, 2641 – 2647, Dec. 1996.

[2] R. Anholt, "Physical compact collector-emitter breakdown model for heterojunction bipolar transistors," *Solid-State Electron.*, vol. 41, pp. 1735 – 1737, Nov. 1997.

[3] R. M. Flitcroft, J. P. R. David, P. A. Houston, Ch. C. Button, "Avalanche multiplication in GaInP/GaAs single heterojunction bipolar transistors," *IEEE Trans. Electron Dev.*, vol. 45, pp. 1207 – 1212, June 1998.

[4] G. Massobrio, P. Antognetti, "Semiconductor Device Modeling with SPICE," New York: McGraw-Hill Book Company, 1993, pp. 32 – 33.

[5] M. Rudolph, R. Doerner, K. Beilenhoff, P. Heymann, "Scalable GaInP/GaAs HBT large-signal model," *IEEE Trans. Microwave Theory Tech.*, vol. 48, pp. 2370 – 2376, Dec. 2000.

[6] M. Rudolph, R. Doerner, K. Beilenhoff, P. Heymann, "Unified model for collector charge in heterojunction bipolar transistors," *IEEE Trans. Microwave Theory Tech.*, vol. 50, pp. 1747 – 1751, July 2002.

[7] M. Achouche, Th. Spitzbart, P. Kurpas, F. Brunner, J. Würfl, G. Tränkle, "High performance InGaP/GaAs HBTs for mobile communications," *Electronics Lett.*, vol. 36, pp. 1073 – 1075, June 2000.

[8] P. Kurpas, F. Brunner, R. Doerner, B. Janke, P. Heymann, A. Maaßdorf, W. Doser, Ph. Auxémery, H. Blanck, D. Pons, J. Würfl, W. Heinrich "High-voltage GaAs power-HBTs for base-station amplifiers" in: *IEEE MTT-S Int. Microwave Symp. Dig.*, 2001, pp. 633 – 636.

[9] P. Baureis, "Electrothermal modeling of multi-emitter heterojunction-bipolartransistors (HBTs)," in: *Dig. INMMC, Workshop on Integrated Non-Linear and Millimeterwave Circuits, Gerhard-Mercator-Universität, Duisburg*, 1994, pp. 145 – 148.

[10] Ch. M. Snowden, „Large-signal microwave characterization of AlGaAs/GaAs HBT's based on a physics-based electrothermal model," *IEEE Trans. Microwave Theory Tech.*, vol. 45, 58 – 71, Jan. 1997.

[11] T. Peyretaillade, M. Perez, S. Mons, R. Sommet, Ph. Auxémery, J. C. Lalaurie, R. Quéré, "A pulsed-measurement based electrothermal model of HBT with thermal stability prediction capabilities," in: *IEEE MTT-S Int. Microwave Symp. Dig.*, 1997, pp. 1515 – 1518.